GlueX Note - 449-v1
Jan 4 2005

Lead Glass and Photomultiplier Evaluation A Progress Report*

Jonathan Dickey, Eric Scott, Paul Smith and Scott Teige
Department of Physics
Indiana University, Bloomington, IN 47405

Abstract

The GlueX collaboration intends to reuse the Lead Glass Detector previously used for Brookhaven National Laboratory Experiment 852. Since lead glass is subject to radiation damage and photomultiplier tubes subject to various aging mechanisms evaluation of the suitability for use of these components is essential. This document describes methods developed and the progress of the evaluation.

Submitted to TJNAF

*Work supported by Department of Energy contract DE-FG02-91ER40661 and Thomas Jefferson National Accelerator Facility

1 Introduction

This note summarizes the activities associated with determination of suitability for GlueX of components of the Brookhaven National Lab E852 Lead Glass Detector. Methods for evaluation and correction of radiation damage of the glass and the operability of the phototubes are presented.

It is found that some of the glass is radiation damaged but the damage can be efficiently reversed. A failure rate of 2.2% for the phototubes is observed.

2 Lead Glass Evaluation

The lead glass was manufactured in Russia and is type F8-00, a type not specifically formulated for radiation resistance. The chemical composition of this glass is 45% PbO, 42.8% SiO_2, 10.4% K_2O and 1.8% Na_2O. It has a density of 3.6 gm/cm^3 and a radiation length of 3.1cm. Its nuclear collision length is 22.5 cm and its index of refraction is 1.62. The dimensions are $4 \times 4 \times 45\, cm^3$. Over 3000 blocks are currently at Indiana University of which 2292 have been subjected to the tests described here.

Radiation exposure causes lead glass to darken, reducing the amount of Cerenkov light produced by electromagnetic showers detected by the phototubes of the calorimeter. Figures 1 and 2 are photographs of damaged and undamaged lead glass blocks.

This radiation damage leads to degradation of the resolution of the detector and is, to some extent, temporary. The damage can also be reversed, at least partially, by exposure to ultraviolet light or heat.

2.1 Evaluation Methods

The radiation damage observed visually can be quantitatively characterized by measurements of the light transmission of the blocks as a function of wavelength and position. A Shimadzu spectrophotometer has been specially modified to allow these measurements to be made. Figure 3 shows the modified spectrophotometer as used for these measurements.

These devices are typically used to measure transmission properties of small, typically liquid, samples of known or unknown chemicals. To use this device for our purposes, a large hole was made in the cavity that normally holds these small samples. The enclosure was enlarged by the addition of an aluminum box with a removable cover. Beneath the spectrophotometer, a mechanical "elevator" was installed to raise and lower the block under test under computer control. This modification allowed the blocks to be scanned along their length. Software was written to allow scans to be conducted under computer control and the data archived automatically.

Figure 4 shows the measured transmission of two blocks as a function of wavelength. One block

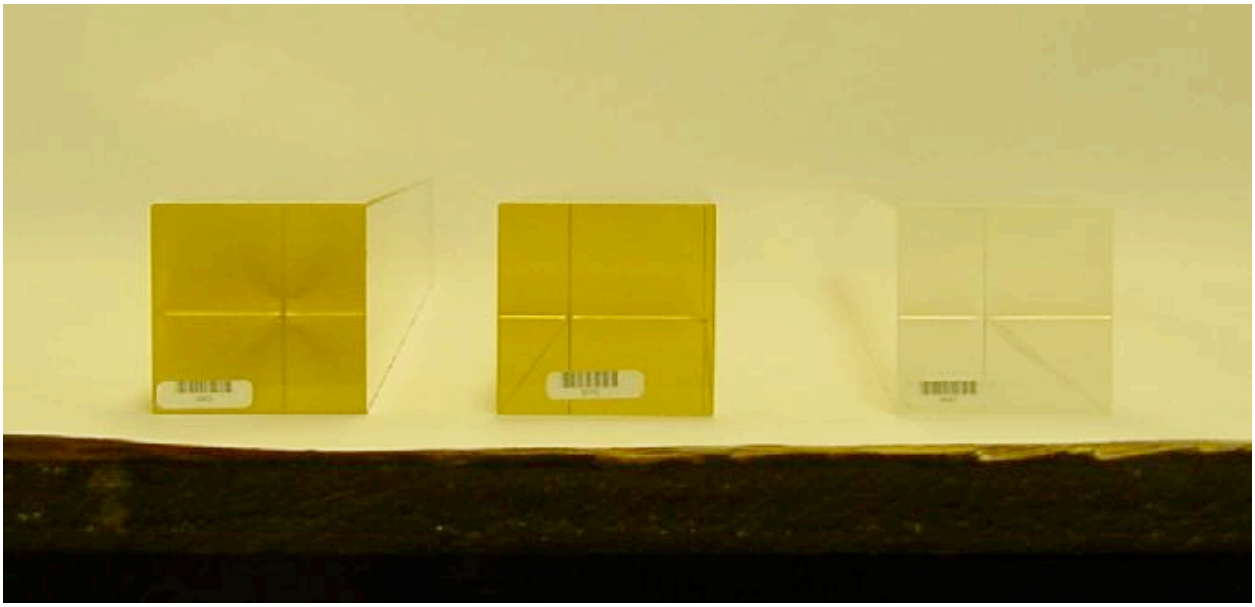

Figure 1: An end view of three blocks. The two at the left were used in RadPhi, the other is from E852. The blocks are $4 \times 4\,cm^2$, the white stickers are bar code lables.

Figure 2: A full length view of one of the damaged blocks. Note the chipped corner on the upper left and the dependence of the damage on the depth into the block

Figure 3: The lead glass testing station. Visible on the left is the modified spectrophotometer. The aluminum structure forms a light-tight enclosure for the block under test. Beneath this (enclosed by the table) is a mechanism that raises and lowers the block under computer control. On the right is the data acquisition/control computer and a table used to unwrap and rewrap blocks before and after testing

had never been used, another was a block selected as slightly radiation damaged. It can be seen that the transmission at shorter (bluer) wavelengths is degraded. Subtraction of blue light leads to a perception of "yellowing" consistent with the visual observations.

In this measurement, and all measurements used for diagnosis of radiation damage, no correction for reflection of light at the surfaces of the glass have been made. The amount of light transmitted at normal incidence across the surface of a transparent material of index of refraction n is given by

$$T = 1 - \left(\frac{n-1}{n+1}\right)^2 . \tag{1}$$

With $n = 1.62$, $T = 94.4\%$. Since two surfaces must be crossed, the expected limiting transmission value for these measurements is T^2 or 89.1%. Examination of figure 4 at long wavelength shows the measurements are consistent with this expectation.

It can also be seen from figure 4 that the fractional change in transmission between damaged and undamaged glass is largest near 410 nanometers. Transmission at this wavelength was chosen as the criterion for selection of damaged/undamaged glass.

The mechanical modifications to the spectrophotometer allow the blocks to be scanned (at one wavelength) along their long dimension. Figure 5 shows the result of one such scan of a radiation damaged block. The units of length in this plot are arbitrary and correspond to a step number in the software controlling the scan.

The data in the figure can be used to determine the conversion algorithm from steps to, for example centimeters. Once this conversion is known, the data can be fitted to determine the characteristic depth of the radiation damage. The transmission is characterized by

$$T = T_0 - Q \exp(-Z/Z_c) \tag{2}$$

where Z_c is the characteristic length of the damage. Z_c is found to be 11 *cm*.

Based on the measurements presented here, the criterion for defining a block as radiation damaged is that transmission at 410 *nm*, uncorrected for reflection, is less than 84%.

2.2 Curing of Radiation Damage

Two methods for reversing the radiation damage were evaluated: Exposure to ultraviolet light and heat treating. Heat treatment was chosen as the preferred method based on the measurements presented below.

2.2.1 UV light

To examine the usefulness of UV curing, a radiation damaged block was exposed to UV light for controlled intervals of time. The transmission was measured after each exposure and fitted to

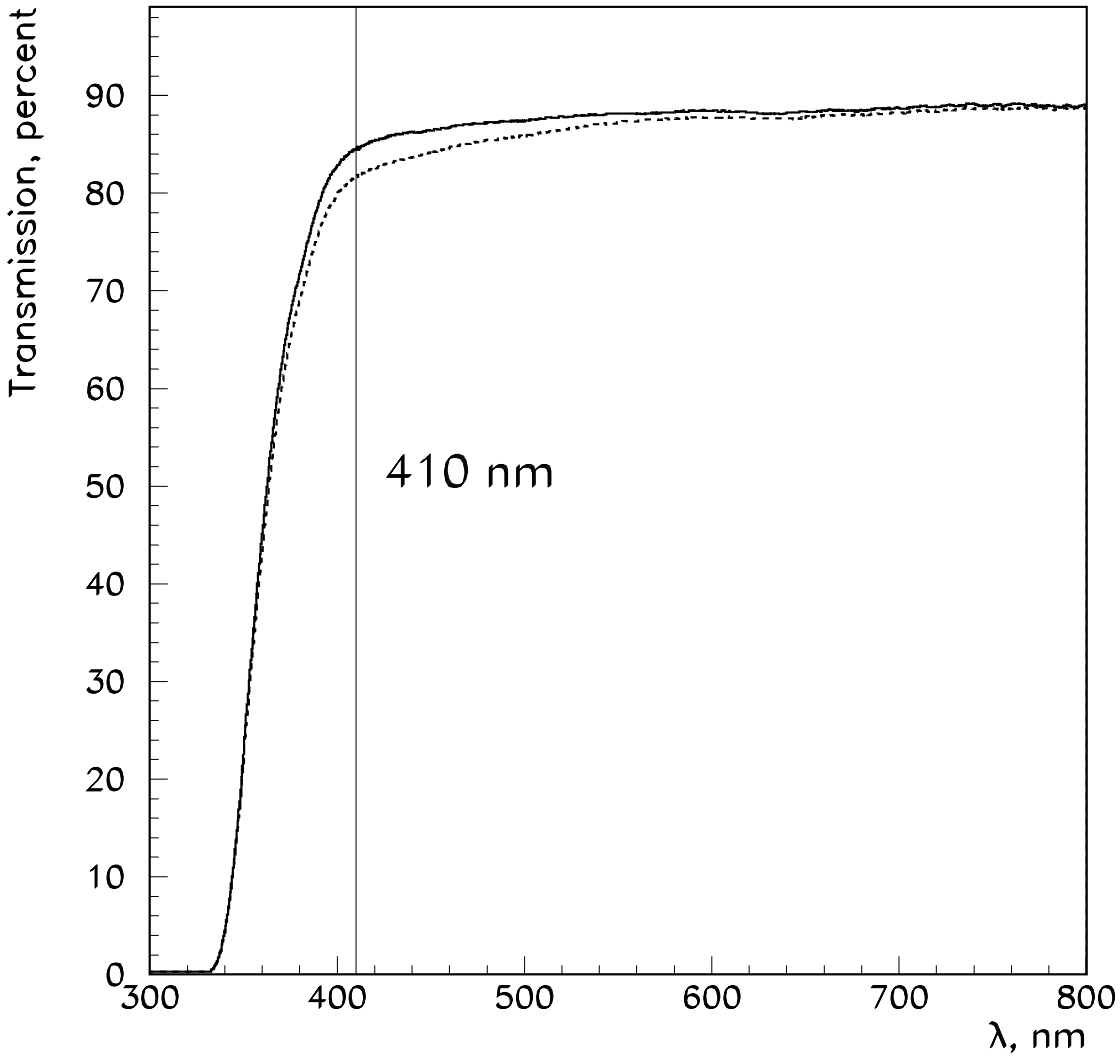

Figure 4: The transmission of unused lead glass (solid curve) and radiation damaged glass (dashed curve) as a function of wavelength. The measurement for the damaged block was made midway along the length of the block, that is, where damage was not easily visually detectable. The line at 410 nm indicates the wavelength chosen to diagnose radiation damage. No corrections for reflection at the surfaces of the glass have been made.

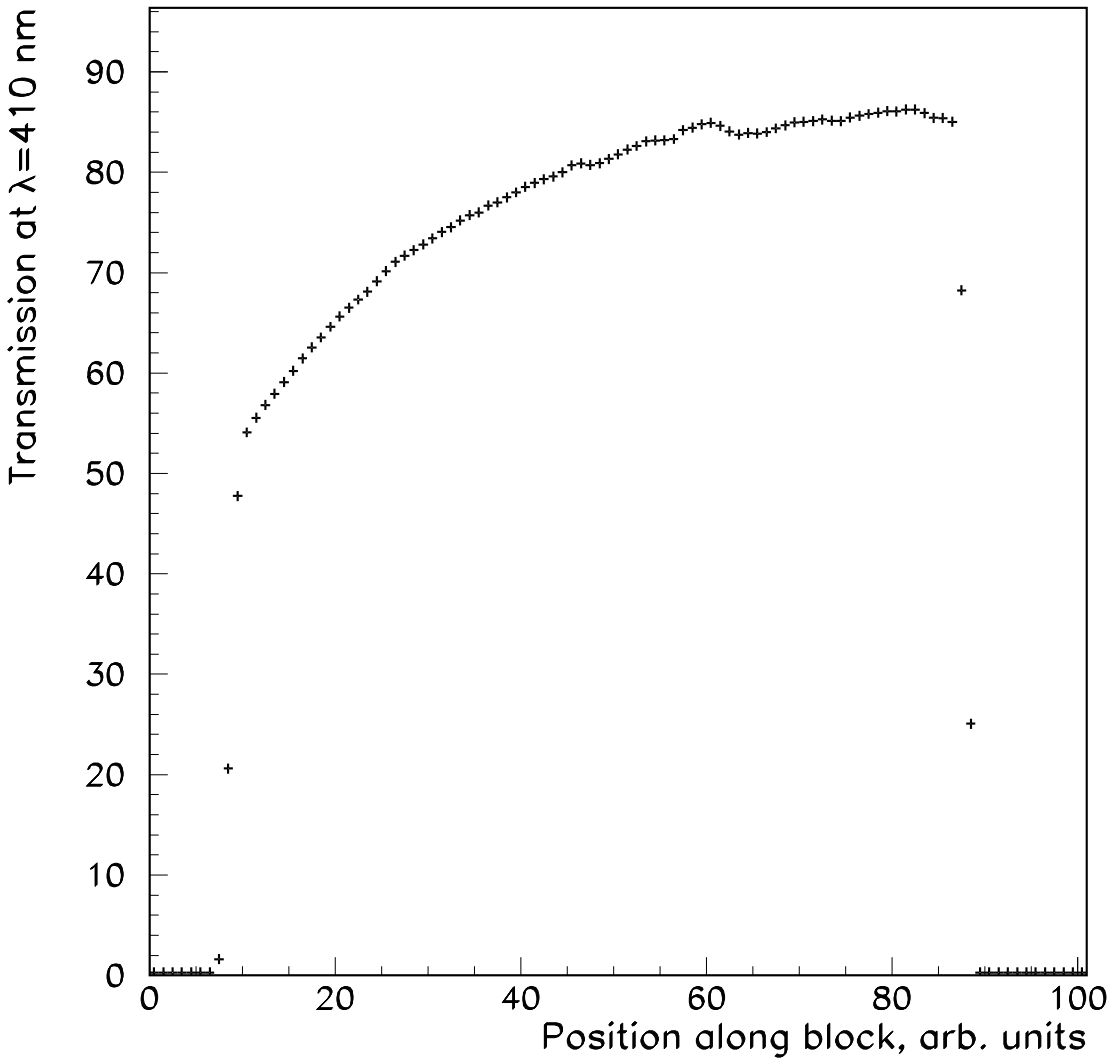

Figure 5: The transmission of 410 *nm* light as a function of depth in a radiation damaged lead glass block. The characteristic length scale of this damage is 11 *cm* or about 3 radiation lengths. No corrections for reflection at the surfaces of the block have been made.

determine the length of time required to complete the cure and the final transmission that could be expected given a cure of infinite length. Figure 6 shows the result of this study for a radiation damaged block. The fit function predicts the transmission that could be achieved if the exposure was carried on forever: 79.8%. This value is substantially smaller than the 89.1% observed for undamaged glass

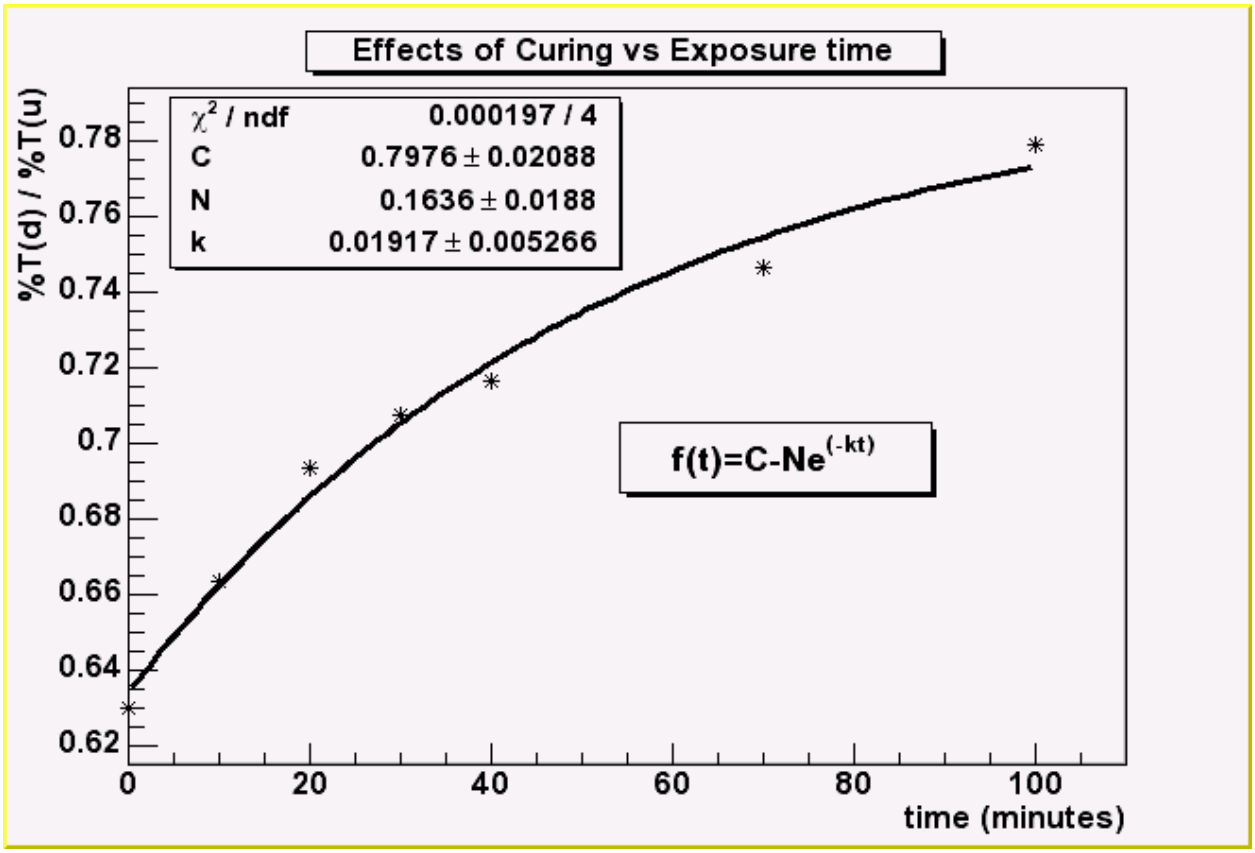

Figure 6: The time dependence of transmission after curing with ultraviolet light

2.2.2 Heat treating

To examine the effects of heat treatment on transmission of radiation damaged blocks a series of measurements were made using some "improvised" equipment. A standard electric kitchen oven was used for these tests.

Because no special temperature controls were used, thermal stressing, associated with uneven heating or sudden changes in conditions, was a concern during this process. To address this issue, an aluminum box was made that could hold two lead glass blocks with about an inch to spare on all sides. The box was partially filled with "agricultural lime", a very finely divided powder available

in large quantities and low cost in the midwest. This dust served two purposes: 1) It isolated the blocks from air currents and 2) served as thermal mass to prevent rapid changes in temperature associated with on/off cycling of the oven.

The blocks were submerged in this dust and placed in the oven. The thermal protection method was tested on several pieces of already broken glass and it was found to work. Several tests using different maximum temperatures were performed and it was determined that the maximum setting of the oven ("Broil") was adequate to completely reverse the radiation damage. The procedure is:

1. Add lime dust to the aluminum container one inch thick
2. Place two blocks to be treated in the container and cover them with dust sufficient to fill the container
3. Place the container into the cold oven, close the door and turn it on to "Broil". Over a period of 2 hours the oven achieves a temperature of 260 degrees C.
4. After 16 hours, (overnight) turn the oven off but do not remove the container with the glass and open the oven door slightly. The oven cools to room temperature over a period of about 3 hours.
5. When the box can be handled, remove the container, unpack the glass and repeat for the next blocks to be treated.

After treatment, the blocks are re-tested. Either visually or using spectrophotometer measurements, heat treated blocks are *indistinguishable* from new lead glass. Figure 7 shows photographs of several treated and untreated blocks. The blocks farthest to the left in this photograph were subjected to the full heat treatment, the others to various lower temperatures. Numerically, the heat treated blocks achieved an uncorrected transmission at 410 nm between 86-87%, identical to values achieved by unused glass.

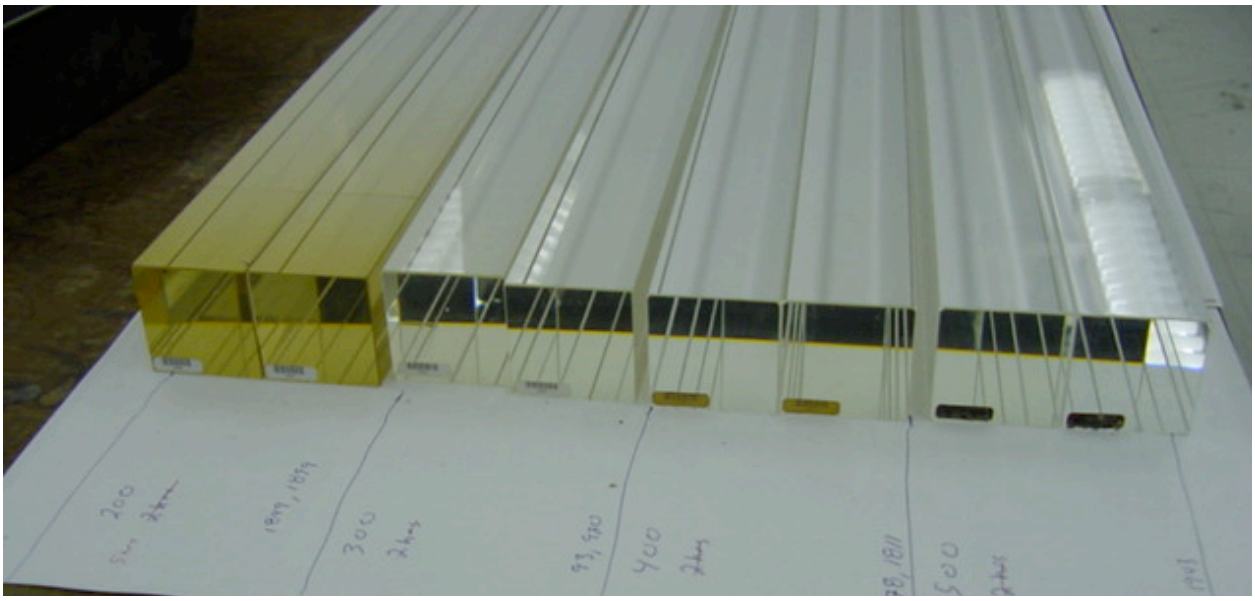

Figure 7: An end view of some representative blocks before and after heat treatment.

3 Photomultiplier Tube Evaluation

3.1 Evaluation methods

Two questions were to be addressed by this study,

1. Do the phototubes still work?
2. Is their noise rate acceptable?

To address these issues a photoube testing station was built. Figure 8 gives a schematic representation of the physical construction of the station. Figures 9 and 10 are photographs of the finished station.

The test station consists of a removable section containing the phototubes, their bases and connectors for signal and high voltage control. Another, fixed section contains a light distribution system consisting of a pair of blue LEDs, a translucent plastic plate to diffuse the light from the LEDs and a light-tight box. A single relay rack contains the data acquisition electronics for the tester.

A technician performs a test cycle for 25 tubes in approximately 1 hour. A test cycle consists of:

1. Removing and unwrapping 25 tubes from their storage container

2. Scanning the bar code of each tube and inserting them sequentially into the bases contained in the removable section of the test station
3. Inserting the removable section into the fixed section
4. Starting the computer controlled test data acquisition process
5. Removing, rewrapping and storing the tested tubes

Data is archived for each tube automatically and analyzed later.

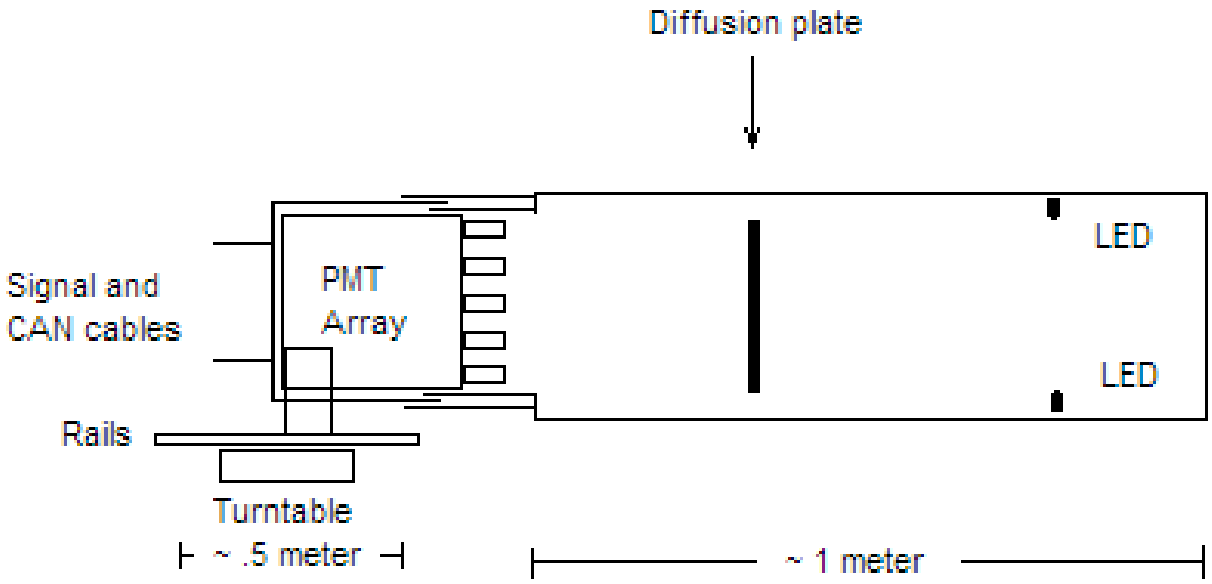

Figure 8: A schematic diagram of the PMT testing station.

3.1.1 Operability

To assess the operability of the tubes, their efficiency as a function of voltage was determined in the following way:

1. The high voltage for all tubes in the tester was set to 1400 volts.
2. The LED was pulsed 1000 times. The pulse duration was 60 ns and the pulse frequency was $\approx 10\,Hz$.
3. A discriminator set to $25mV$ determined if a signal was present in the tube or not. The output of the discriminator in coincidence with the LED triggered a scaler for each channel.

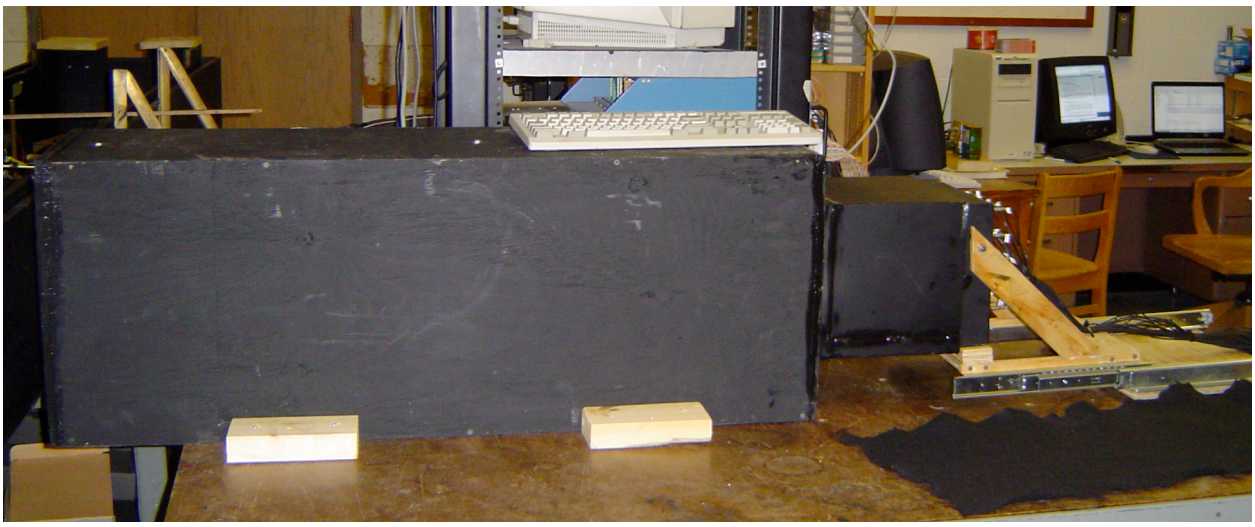

Figure 9: PMT test station, closed position

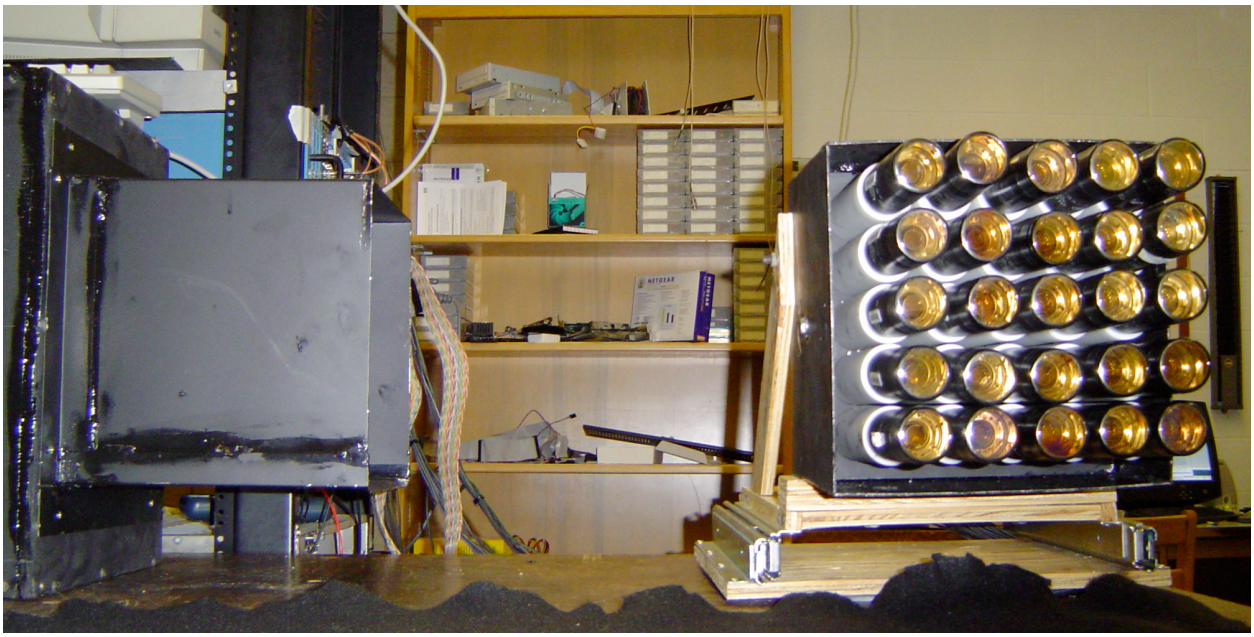

Figure 10: PMT test station, open position

4. After the 1000 LED pulses, the contents of the 25 scaler channels was recorded
5. The voltage was increased by 20 volts, the scalers reset and the test repeated.
6. The test was terminated after a measurement at 1900 volts was performed

Figure 11 shows the number of scaler counts as a function of voltage for a typical tube.

The smooth curve in figure 11 is given by

$$N = \frac{1}{2}N\left(1 + \mathrm{erf}\left\{\frac{V - V_0}{\sqrt{2}\sigma}\right\}\right). \tag{3}$$

The parameters N, V_0 and σ are determined on a tube by tube basis by a fit to the data. V_0 is the voltage where eqn. 3 achieves a value[†] of $N/2$, that is, where the tube is 50% efficient. The parameter σ measures the width of the rise of the curve. A typical value for σ is about 20 Volts. For the tube shown in figure 11 the 50% voltage was found to be 1588 volts. Shown in figure 12 is the distribution of values found for V_0.

The data from the tester was analyzed offline. A tube was flagged as "suspect" if the function given by 3 failed to reach 90% efficiency over the tested range of voltages. Diagnostic output was printed to the screen identifying the tube and giving the location of further diagnostic data. The distributions shown in figure 11 for flagged tubes were examined. About 10% of all tested tubes were initially flagged by this process. The detailed examination revealed that most flagged tubes were, in fact, operational but the fit failed to converge. In nearly all cases this failure to converge was caused by a "late turn on" of the phototube response. That is, the 50% voltage was in excess of ≈ 1850 volts. The fit was initialized so that it would converge for most tubes thereby minimizing the number of distributions to be examined in detail. However, this choice of initialization resulted in the $\approx 10\%$ false positive test rate.

Determination of failure during detailed examination was unambiguous. The tubes detected as failures had *no* signals over threshold at any voltage. Of the 977 tubes tested to date, 21, or 2.2% have failed. The failed tubes were inspected visually to determine if this method would be sufficient to detect failed tubes. 9 of the failed tubes had the transparent photochathode characteristic of vacuum failure. One of these was mechanically damaged, a crack in the envelope was apparent.

3.1.2 Noise rates

Phototubes exhibit several types of noise: correlated noise and dark noise. Correlated noise is pulsing not associated with light on the photocathode after a real pulse caused by light. Dark noise is random pulsing when the tube is under high voltage and not exposed to light. Methods to determine these quantities are being developed, implemented and a report generated when reliable measurements are available. Below we show preliminary data that numerically defines these noise rates.

[†]The error function has a range of -1 to 1 over its domain from $-\infty$ to $+\infty$

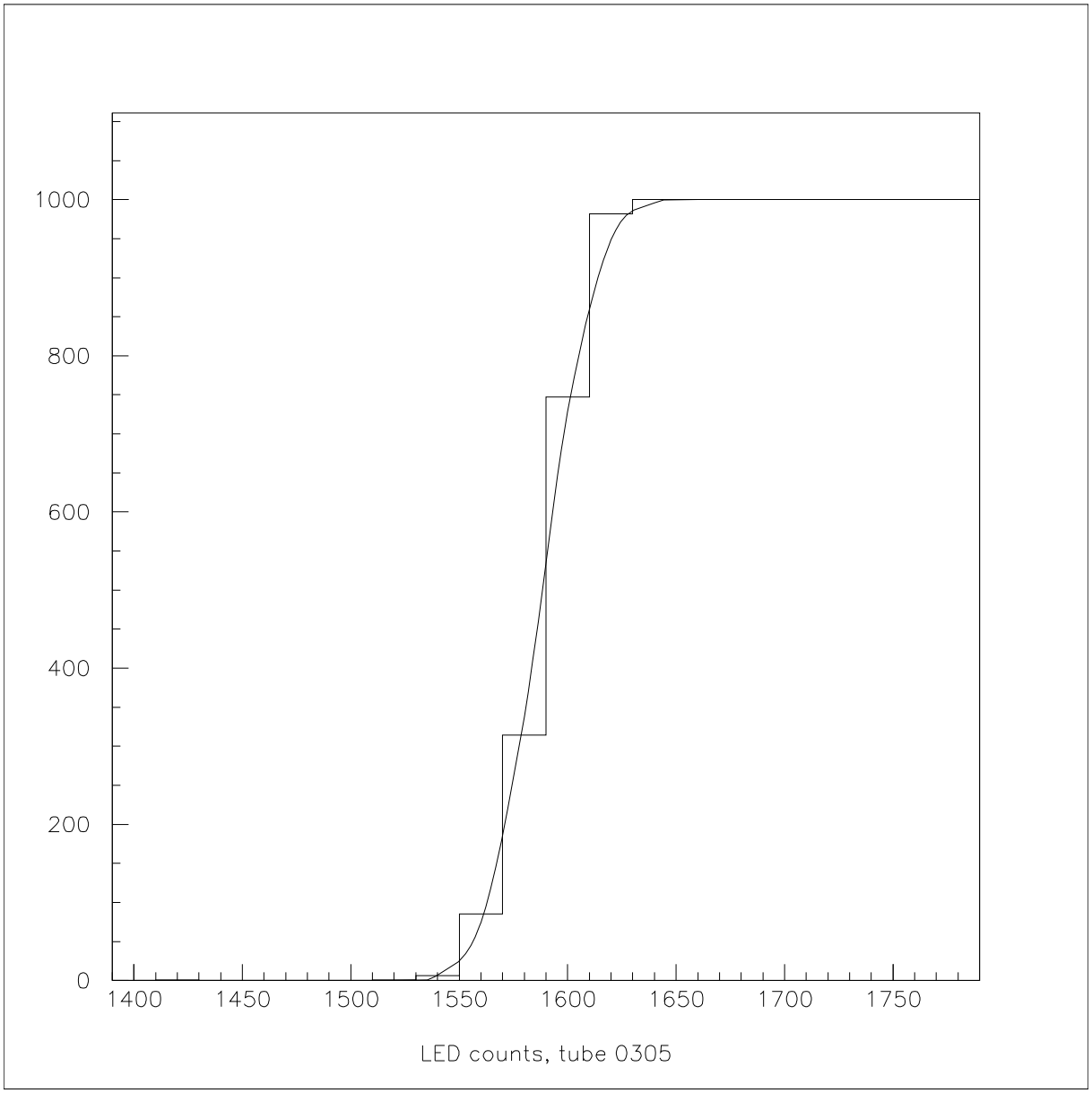

Figure 11: The response of a tube to the LED as a function of voltage. On the vertical axis is the number of times the tube had a pulse over threshold associated with an LED pulse. The LED was pulsed 1000 times at each voltage. The smooth curve is a fit to the data and gives the voltage where the PMT was 50% efficient.

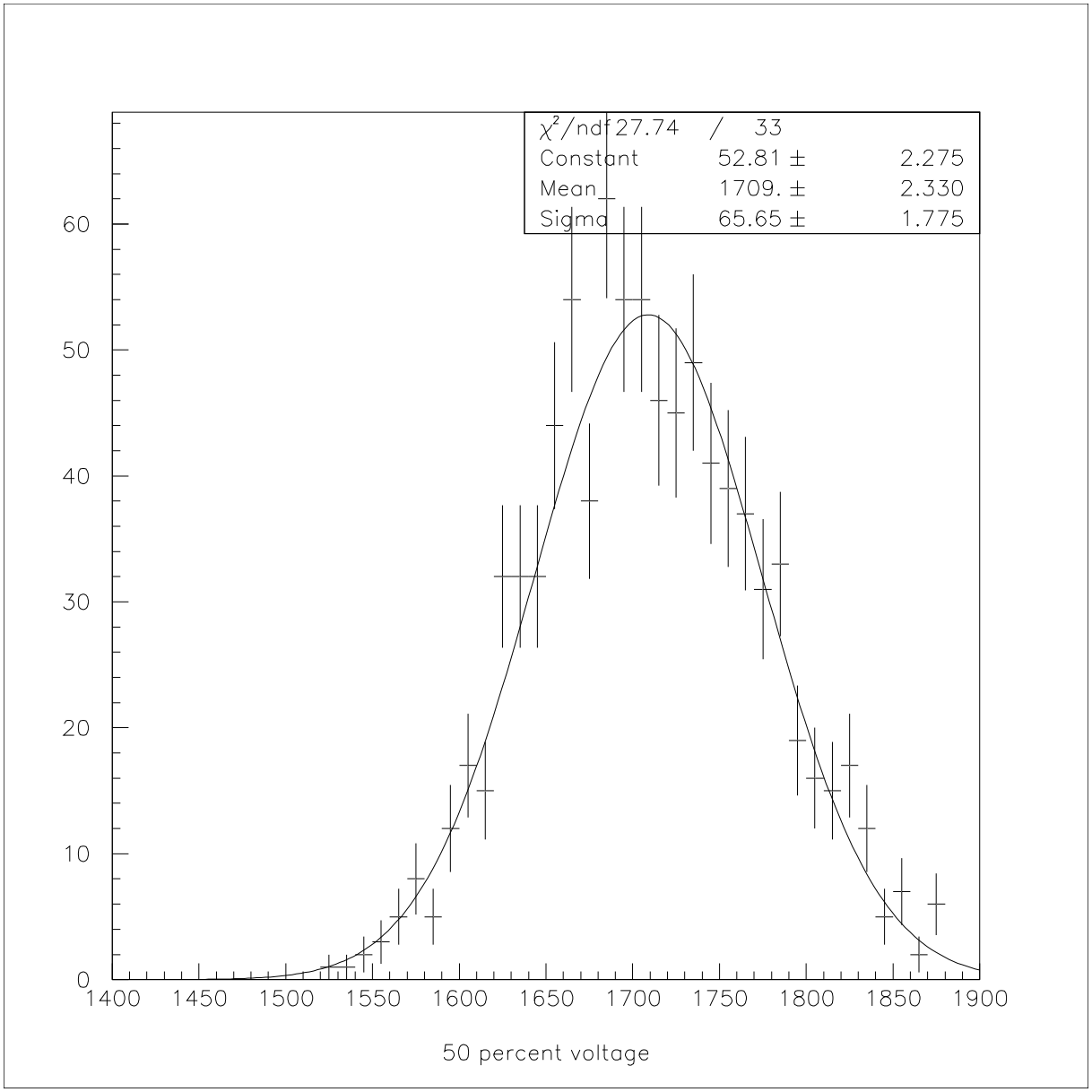

Figure 12: The observed distribution of V_0 for the tubes tested to date.

Figure 13 shows a correlated noise measurement for a single phototube. The procedure for obtaining this data was as follows:

1. The tube was raised to an voltage typical of operating voltages for tubes of this type, in this case 1900V.
2. The tube was illuminated by an LED pulse with a duration of 60 *ns*
3. After a period of delay, a discriminator was gated for 600 *ns*. The number of pulses over a threshold of 20 mV was recorded by a scaler
4. The total number of after-pulses for 1000 LED pulses is recorded and the delay of the start of the scaler gate is changed

The average number of after-pulses in the 600 *ns* window pulses as a function of the start time of the gate is shown in figure 13. The after-pulsing rate is seen to decay exponentially. A fit to the data gives a characteristic time for this decay of 470 *ns*.

Figure 14 shows a dark noise measurement for a single phototube. It is often asserted that dark noise decreases after a phototube is kept in darkness for some period of time. Shown is the dark noise rate measured for a phototube after exposure to fluorescent light as a function of time since the exposure. The data is fitted to a function of the form

$$R = C + R_0 \exp\left(\frac{-t}{t_d}\right) \tag{4}$$

where C is the dark noise rate at infinite time and t_d is the characteristic decay time for the noise rate. It is clearly seen that the dark noise rate approaches a limiting value after a period of about two hours.

The data from the phototube tester is currently being evaluated to develop a method to characterize the noise properties of the phototubes.

4 Conclusions

- Methods to evaluate the transmission of lead glass have been developed and these methods used to diagnose the existence of radiation damage.
- Two methods to reverse radiation damage in lead glass have been evaluated. It has been demonstrated that heat treating is superior to curing with ultraviolet light.
- A method to quantitatively determine the efficiency of a photomultiplier tube as a function of voltage has been developed and used to diagnose a failure mode. The PMT failure rate to this mode is 2.2%

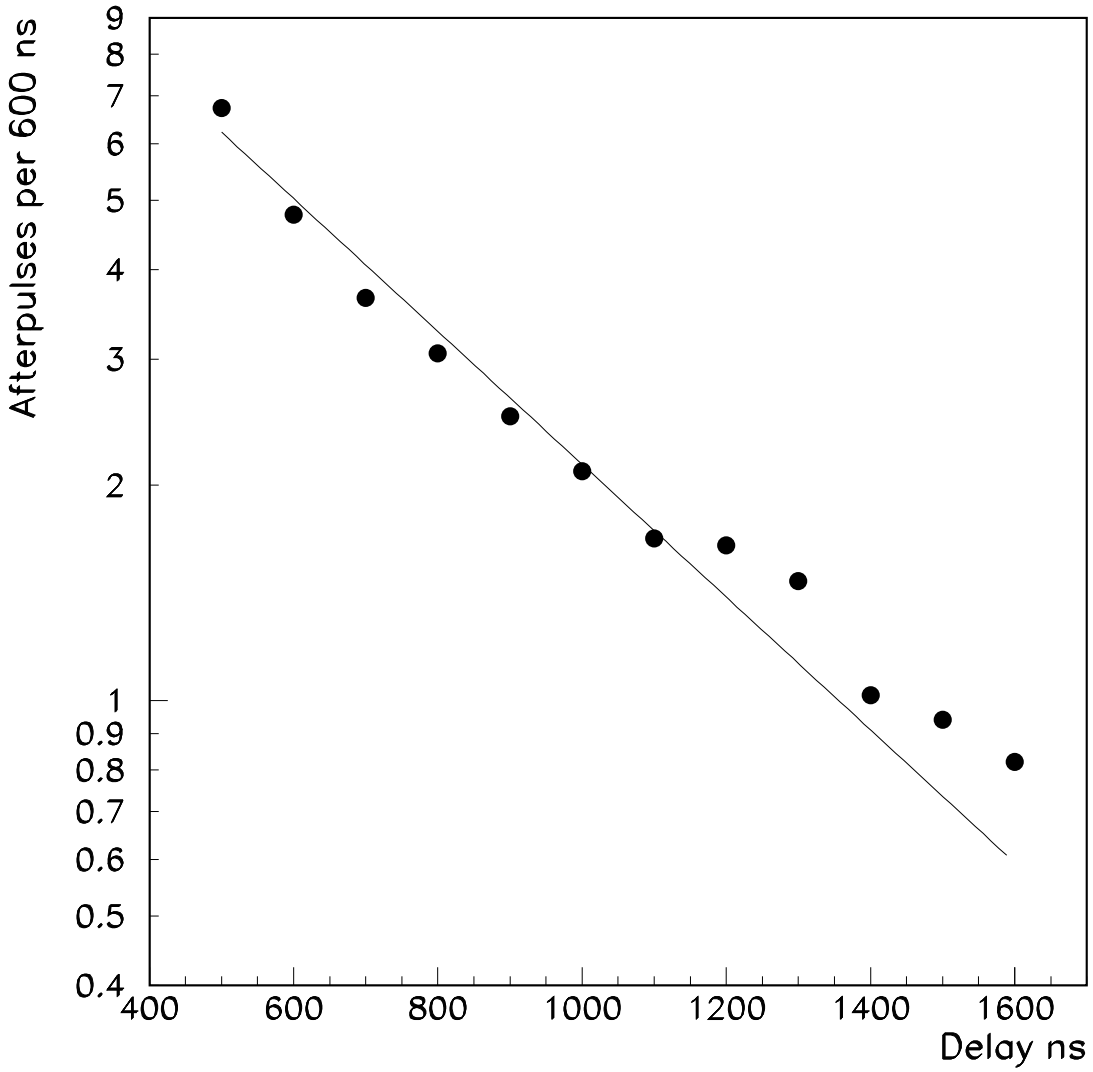

Figure 13: After-pulsing rate as a function of gate start time from the initial pulse. A decay constant of 470 ns is obtained from a fit to the data.

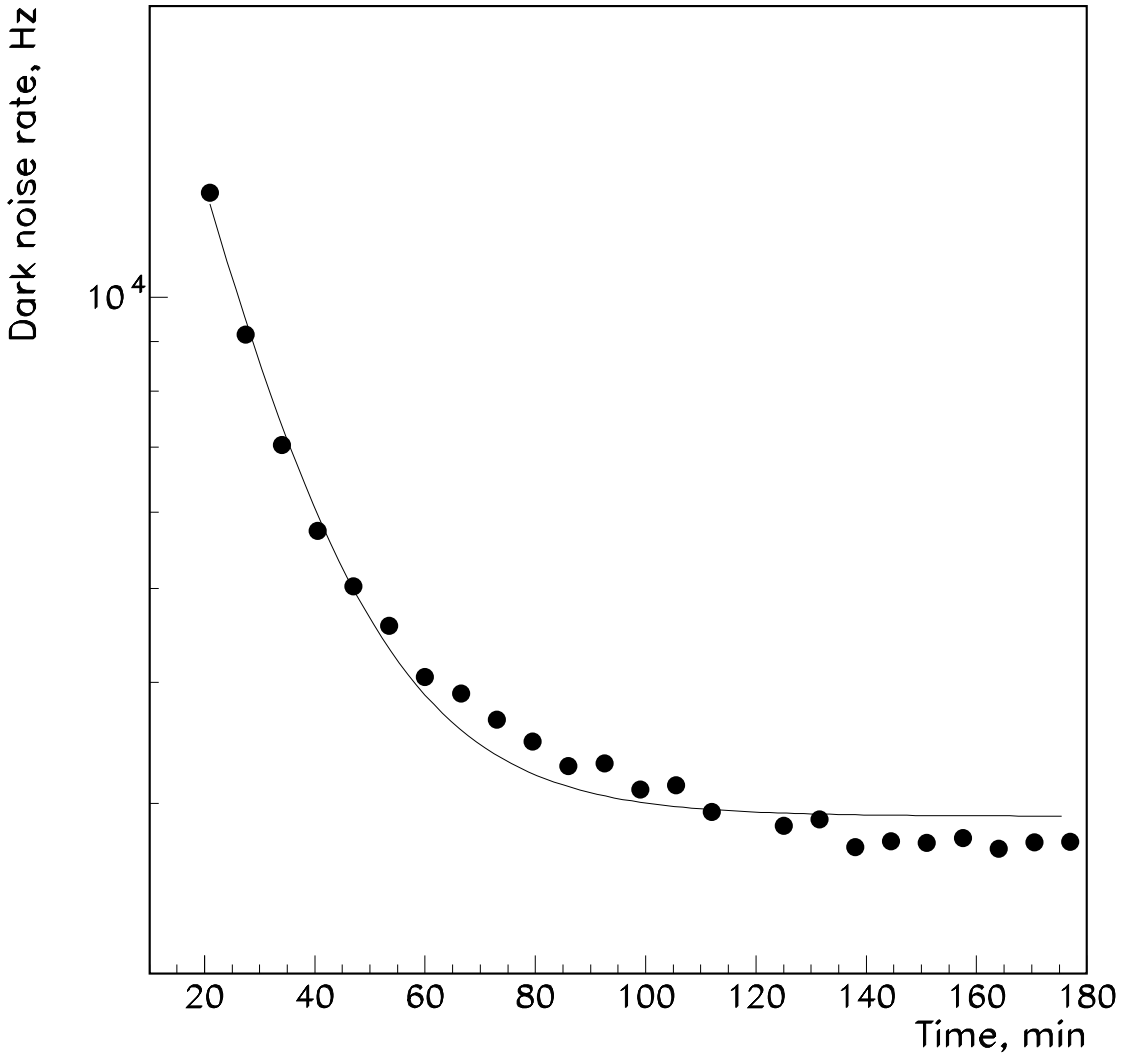

Figure 14: Dark noise rate as a function of the length of time the tube was under voltage and in the dark. A decay constant of ≈ 17 minutes is obtained from a fit to the data.